Graphoepitaxial high-T_c SQUIDs

2014 J. Phys.: Conf. Ser. 507 042009

(http://iopscience.iop.org/1742-6596/507/4/042009)

Journal of Physics: Conference Series **507** (2014) 042009 doi:10.1088/1742-6596/507/4/042009

Graphoepitaxial high-T_c SQUIDs

M. I. Faley[1], **D. Meertens, U. Poppe and R. E. Dunin-Borkowski**
Peter Grünberg Institute (PGI-5: Microstructure Research)
Forschungszentrum Jülich GmbH, D-52425 Jülich, Germany

E-mail: m.faley@fz-juelich.de

Abstract. The fabrication process and physical properties of graphoepitaxially engineered high-T_c direct current superconducting quantum interferometer devices (DC SQUIDs) are studied. Double buffer layers, each comprising a graphoepitaxial seed layer of $YBa_2Cu_3O_{7-x}$ and an epitaxial blocking layer of $SrTiO_3$, were deposited over textured step edges on (001) surfaces of MgO substrates. Scanning electron microscopy and high-resolution transmission electron microscopy were used to investigate the microstructural properties of DC SQUIDs with graphoepitaxial Josephson junctions. Both direct coupled and inductively coupled high-T_c DC SQUIDs with graphoepitaxial step edge junctions and flux transformers were studied.

1. Introduction

High-T_c thin film superconducting devices utilize the unique properties of macroscopic quantum phenomena in superconductors and much lower cryogenic costs for their operation at 77 K, when compared to low-T_c devices, which are affected by the increasing cost of liquid helium. However, the low noise performance of high-T_c circuits requires sophisticated engineering of the microstructures of the films and Josephson junctions, taking into account the $d_{x^2-y^2}$ pairing symmetry of the superconducting gap function and the short coherence length in high-T_c superconductors. A single grain boundary in a high-T_c film that has been fabricated on a properly prepared substrate surface can serve as a high quality Josephson junction. Step edge Josephson junctions are cheaper in production when compared to ramp- and bicrystal Josephson junctions and demonstrate excellent superconducting parameters [1-4]. The reproducibility of step edge junctions can be improved using multilayer epitaxial buffering of step edges. Epitaxially buffered MgO substrates [5] are advantageous for the growth of $YBa_2Cu_3O_{7-x}$ (YBCO) films due to the similar thermal expansion coefficients of MgO and YBCO. Epitaxial buffers can also be used to improve the growth of YBCO films over the step edges: enhanced graphoepitaxial growth of YBCO films on a texturing layer with an artificially created micro-relief on the surface steps of MgO substrates has been proposed and verified [4, 6, 7]. These Josephson junctions were intended for integration in high-T_c direct current superconducting quantum interference devices (high-T_c DC SQUIDs). Such SQUIDs can be used, for example, in measurement systems for low field magnetic resonance imaging, geomagnetic surveys or magnetoencephalography (MEG). In the present paper, we describe high-T_c DC SQUIDs prepared with an additional epitaxial buffer layer of $SrTiO_3$ (STO), which serves as a blocking barrier against possible contamination of the superconducting YBCO film as a result of diffusion of Mg from the MgO substrate [8].

[1] Corresponding author. E-mail address: m.faley@fz-juelich.de.

2. Experimental details

Heterostructures of Josephson junctions and DC SQUID magnetometers were deposited by high-oxygen-pressure magnetron sputtering from stoichiometric polycrystalline targets [9, 10]. The formation of steps on MgO substrates was performed by ion beam etching (IBE) at an incident angle of 45° over the edge of an AZ TX1311 photoresist reflowed to achieve a 45° slope angle. The photoresist was removed using acetone and methanol. A second IBE step was used at an incident angle of 90° to clean the surface of fences of resputtered material [11] and to make an initial texture in the form of linear trenches along the [100] and [010] directions of the MgO substrate [4]. Enhancement of the texture was achieved by depositing a 10 nm thick homoepitaxial MgO film [12]. This texture was used to achieve graphoepitaxial growth of the YBCO films, resulting in an in-plane orientation of the YBCO films on the step edge and on the rest of the substrate surface. Contamination of the YBCO film and grain boundaries by Mg from the MgO substrate [8] was avoided by using an epitaxial blocking layer of STO of thickness about 30 nm deposited above a 10 nm thick YBCO seed layer. Atomic force microscopy (AFM), scanning electron microscopy (SEM) and high-resolution transmission electron microscopy (HRTEM) were used to characterise the textured surfaces of the step edges and the microstructure of the films. In-plane alignment of the grains in the YBCO films was confirmed by observing the orientations of growth spirals on the film surfaces using AFM and SEM.

The DC SQUIDs were made from the YBCO-STO-YBCO heterostructures and each consisted of two 2-μm-wide step-edge Josephson junctions. Multilayer superconducting flux transformers for inductively coupled SQUID magnetometers were prepared using YBCO, $PrBa_2Cu_3O_{7-x}$ and STO films on single crystal MgO (001) wafers buffered by epitaxial $BaZrO_3$ and STO films and assembled in a flip-chip geometry with the DC SQUIDs.

3. Results and discussion

HRTEM images of an YBCO-STO-YBCO heterostructure deposited on a textured step edge on an MgO substrate is shown in Fig. 1. The lower YBCO layer serves only as a seed layer and was not superconducting at 77 K due to contamination by Mg atoms sustained during deposition of the YBCO. Thanks to the use of the STO blocking layer, the superconducting transition temperature T_c of the top YBCO layer increased from approximately 89 K to above 91 K. Similar to the results obtained in Ref. [4], two [100]-tilted 45°-misoriented grain boundaries were observed at each step edge junction.

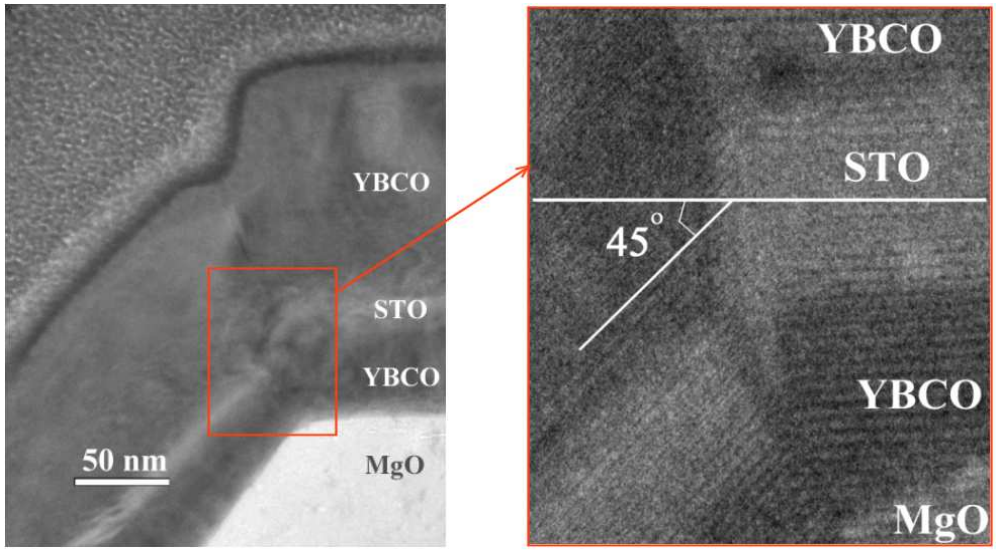

Figure 1. HRTEM images of an YBCO-STO-YBCO heterostructure deposited on the top corner of a textured step edge on an MgO substrate.

The implementation of the surface texture changed the growth mode of the YBCO film on the MgO surface from epitaxial to graphoepitaxial, resulting in alignment of the in-plane orientation of the YBCO film on the substrate steps. The orientation of the growth spirals showed that all of the grains in the YBCO film were aligned in-plane, with their *a*- or *b*- axes normal to the step. This property was reflected in improved reproducibility and improved parameters of the step-edge Josephson junctions made by patterning 2 μm wide bridges in the YBCO films across the steps. The I-V characteristics of the Josephson junctions showed RSJ-like behavior, with negligible excess supercurrent and values of I_cR_n product of approximately 0.6 mV at 77 K.

The high value of the I_cR_n product observed in the graphoepitaxial Josephson junctions can be explained by the fact that the grain boundaries in these junctions are straight, leading to a more homogeneous distribution of the Josephson current compared to that in [001]-tilted bicrystal junctions and to step edge junctions without in-plane alignment of the grains. In addition, Andreev bound quasiparticle states at the midgap energy (zero-energy states) probably do not appear in the case of a [100]-tilted grain boundary junctions [13]. These states could otherwise be responsible for partial electrical shunting of the resistance and for deviation of the critical current from the Sigrist–Rice phenomenological approach [14] in the case of [001]-tilted grain boundary junctions.

Step edge junctions provide much more freedom with regard to their positioning on the substrate, when compared to bicrystal junctions. Also, the steps on the substrate can be placed so that they influence the YBCO films only in the areas of the Josephson junctions, with the rest of the YBCO films remaining unperturbed and retaining the highest critical current and lowest noise values. These features are advantageous for the construction of both direct coupled DC SQUIDs (see Fig. 2) and also SQUIDs that are inductively coupled to superconducting flux transformers with multiturn input coils, due to the improved availability and lower costs of the substrates, improved reproducibility of the Josephson junctions due to a smaller concentration of voids, higher I_cR_n product, lower junction capacitance and easier alignment during photolithography, when compared with bicrystal junctions.

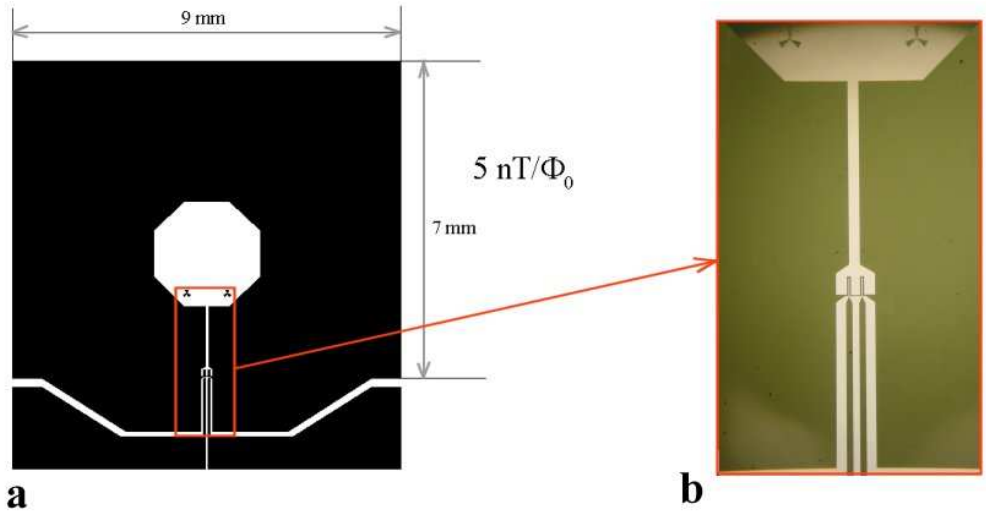

Figure 2. (a) Sketch of a direct coupled high-T_c DC SQUID magnetometer with an 8 mm pick-up loop and step edge Josephson junctions. (b) Photograph of the inner part of the magnetometer with two DC SQUIDs. Each SQUID has an inductance of approximately 100 pH.

Figure 2 shows a sketch and a photograph of a direct coupled DC SQUID magnetometer with step edge Josephson junctions prepared on a 10 mm x 10 mm MgO substrate. The SQUID magnetometer consists of a 9 mm x 7 mm pick-up loop and two DC SQUIDs. Each DC SQUID has a loop inductance of approximately 100 pH, according to estimates made with the help of the software package 3D-MLSI [15]. Such direct coupled DC SQUID magnetometers with graphoepitaxial step

edge Josephson junctions demonstrated an ~ 5 nT/Φ_0 field-to-flux transformation coefficient and a magnetic field resolution of ~ 50 fT/√Hz at 77 K.

An increase in the size of the pick-up loop to about 25 mm leads to an improvement in the field-to-flux transformation coefficient to approximately 1.5 nT/Φ_0, and to a magnetic field resolution of ~ 15 fT/√Hz at 1 kHz and 77 K. This value is comparable to that reported in Ref. [16] for similar frequency and temperature conditions. A moderate improvement of sensitivities can be obtained by inductive coupling of the direct coupled SQUIDs to single layer flux transformers made from relatively thick superconducting films [5]. Such coupling leads also to a reduction in the pick-up loop inductance, which improves the sensitivity and operational stability of the sensor even if the flux concentrator has a similar area to that of the pick-up loop of the SQUID.

Much greater sensitivity improvement was achieved by the implementation of inductive coupling of the SQUIDs to a multiturn input coil of 8-mm or 16-mm superconducting flux transformers [17]. Magnetometers with 8-mm flux transformers demonstrated field-to-flux transformation coefficient of approximately 1.2 nT/Φ_0 and magnetic field resolution of ~ 12 fT/√Hz at 77 K. Magnetometers with 16-mm flux transformers observed field-to-flux transformation coefficients of ~ 0.45 nT/Φ_0 and magnetic field resolutions of ~ 5 fT/√Hz at 77 K. The noise spectrum of these magnetometers was white down to the frequencies of about 10 Hz and achieved of ~ 20 fT/√Hz at 1 Hz.

Acknowledgments

The authors gratefully acknowledge fruitful discussions with Yu. V. Maslennikov, A. S. Sobolev, G. A. Ovsyannikov and V. P. Koshelets and the technical assistance of V. Yu. Slobodchikov and R. Speen. The authors acknowledge IB-BMBF (project 01DJ13014) for partial financial support.

4. References

[1] Daly K P, Dozier W D, Burch J F, Coons S B, Hu F L, Platt C E, and Simon R. W 1991 *Appl. Phys. Lett*. **58**, 543
[2] Jia C L, Kabius B, Urban K, Herrmann K, Schubert J, Zander W, and Braginski A I 1992 *Physica C* **196** 211
[3] Foley C P, Lam S, Sankrithyan B, and Wilson Y 1997 *IEEE Trans. Appl. Superconductivity* **7** 3185
[4] Faley M I, Poppe U, Dunin-Borkowski R E, Schiek M, Boers F, Chocholacs H, Dammers J, Eich E, Shah N J, Ermakov A, Slobodchikov V Yu, Maslennikov Yu V, and Koshelets V P 2013 *IEEE Transactions on Appl. Supercond*. **23** 1600705
[5] Faley M I, Mi S B, Petraru A, Jia C L, Poppe U, and Urban K 2006 *Appl. Phys. Lett*. **89** 082507
[6] Faley M I 2012 Reproduzierbarer Stufen-Josephson-Kontakt *Patent pending DE102012006825*
[7] Faley M I, Meertens D, Poppe U, and Dunin-Borkowski R E 2013 *Extended abstracts of 14th International Superconductive Electronics Conference (ISEC 2013)* 247-249
[8] Hao Z, Wu Y, Enomoto Y, Tanabe K, and Koshizuka N 2002 *Journal of Appl. Phys*. **91** 9251
[9] Poppe U, Klein N, Dähne U, Soltner H, Jia C L, Kabius B, Urban K, Lubig A, Schmidt K, Hensen S, Orbach S, Müller G, and Piel H 1992 *J. Appl. Phys*. **71** 5572
[10] Faley M I, and Poppe U 2012 *Patent* WO2012051980
[11] Mitchell E E and Foley C P 2010 *Supercond. Sci. Technol*. **23** 065007
[12] Copetti C A, Schubert J, Klushin A M, Bauer S, Zander W, Buchal Ch, Seo J W, Sanchez F, Bauer M 1995 *J. Appl. Phys*. 78 5058
[13] Löfwander T, Shumeiko V S, and Wendin G 2001 *Supercond. Sci. Technol.* **14** R53
[14] Barone A, Lombardi F, Monaco A, Sarnelli E, Tafuri F, and Testa G 2004 *Phys. Stat. Sol. (b)* **241** 1192
[15] Khapaev M M, Kupriyanov M Yu, Goldobin E, Siegel M 2003 *Supercond. Sci. Technol*. **16** 24
[16] Lee L P, Teepe M, Vinetskiy V, Cantor R, and Colclough M S 1995 *Appl Phys Lett*. **66** 3058
[17] Faley M I, Poppe U, Urban K, Paulson D N, Starr T, and Fagaly R L 2001 *IEEE Transactions on Appl. Supercond*., **11** 1383